Chinese Journal of Aeronautics, 2013,26(3): 563–571

Chinese Society of Aeronautics and Astronautics
& Beihang University

Chinese Journal of Aeronautics

cja@buaa.edu.cn
www.sciencedirect.com

Numerical study of unsteady starting characteristics of a hypersonic inlet

Wang Weixing, Guo Rongwei *

College of Energy and Power Engineering, Nanjing University of Aeronautics and Astronautics, Nanjing 210016, China

Received 26 December 2011; revised 27 March 2012; accepted 27 July 2012
Available online 2 May 2013

KEYWORDS

Hypersonic flow;
Inlet;
Scramjet;
Start;
Unsteady

Abstract The impulse and self starting characteristics of a mixed-compression hypersonic inlet designed at Mach number of 6.5 are studied by applying the unsteady computational fluid dynamics (CFD) method. The full Navier–Stokes equations are solved with the assumption of viscous perfect gas model, and the shear-stress transport (SST) k–ω two-equation Reynolds averaged Navier–Stokes (RANS) model is used for turbulence modeling. Results indicate that during impulse starting, the flow field is divided into three zones with different aerodynamic parameters by primary shock and upstream-facing shock. The separation bubble on the shoulder of ramp undergoes a generating, growing, swallowing and disappearing process in sequence. But a separation bubble at the entrance of inlet exists until the freestream velocity is accelerated to the starting Mach number during self starting. The mass flux distribution of flow field is non-uniform because of the interaction between shock and boundary layer, so that the mass flow rate at throat is unsteady during impulse starting. The duration of impulse starting process increases almost linearly with the decrease of freestream Mach number but rises abruptly when the freestream Mach number approaches the starting Mach number. The accelerating performance of booster almost has no influence on the self starting ability of hypersonic inlet.

1. Introduction

As the main compression component of a hypersonic propulsion system, the inlet affects the performance of scramjet greatly. The mixed-compression type, which may cause starting problem, is always employed in hypersonic inlet in order to obtain better aerodynamic performance. The starting problem is inherent to internal compression duct because the structure does not allow surplus mass flow to spill overboard.[1] The starting characteristics of a hypersonic inlet determine directly the flight envelope of aerocraft, so a variety of methods have been developed to prevent the inlet from unstarted mode and extend its stable operation envelope.

Over the past few decades, the starting problems of hypersonic inlet have been studied extensively.[2–11] Efforts have been made to understand the flow pattern at unstarted mode and explore the approaches of widening the flight envelope of hypersonic inlet. Mass flow spillage[12,13] and overspeeding[14] have been contrived to overcome the Kantrowitz limit, but these

* Corresponding author. Tel.: +86 25 84892444.
E-mail addresses: wwxbaby@163.com (W. Wang), guoweifang@nuaa.edu.cn (R. Guo).

Peer review under responsibility of Editorial Committe of CJA.

ELSEVIER Production and hosting by Elsevier

1000-9361 © 2013 Production and hosting by Elsevier Ltd. on behalf of CSAA & BUAA. Open access under CC BY-NC-ND license.
http://dx.doi.org/10.1016/j.cja.2013.04.018

methods are considerably difficult to implement in scramjet inlet from a practical point of view. More viable methods can be categorized into two major classes[15] variable geometries and unsteady effects. The former approach improves the inlet starting ability through regulating the mass flow entry and the area of throat.[16] The latter approach makes use of highly unsteady effects to overcome the Kantrowitz limit.[1,17] Compared with variable geometry inlet, the structure of fixed geometry inlet is simple. So the unsteady effects are a better method to improve the starting ability of a fixed geometry inlet.

The unsteady starting characteristics of inlet have been studied numerically. Tahir et al.[14] has studied the unsteady starting process of inward turning supersonic inlets numerically, and the evolvement process of the flow field is described in detail. The results indicate that the removal of frangible structures such as sudden rupturing diaphragms may be employed near the leading edge of an inlet to sufficiently impose high spatial gradients, so as to permit starting beyond Kantrowitz's limit. The higher ratio initial values of external to internal pressure are conducive to unsteady starting. But this paper assumes that the gas is inviscid and neglects the viscous influence on inlet starting. The viscous influence on the unsteady starting is considered in Ref. [15], and the starting approaches of opening doors, rocket plugs and sliding doors are employed. Comparative analyses are conducted on the evolvement of flow field of inlet with different starting approaches, and the results indicate that the better starting capability could be obtained with the approach of sliding doors. However, these works mainly focus on the pure internal compression inlet and the unsteady starting process of inlet with different approaches. The unsteady starting characteristics of inlet in impulse wind tunnel, during which the unsteady starting shock of impulse wind tunnel will sweep the inlet, are not referred to.

Different from a bow shock standing ahead the pure internal compression inlet, an oblique shock generated by cowl will shoot into the internal compression duct of a mixed-compression inlet, which would benefit overcoming the Kantrowitz limit. The unsteady starting characteristics of mixed-compression hypersonic inlet in impulse wind tunnel and self starting process will be discussed in this paper.

2. Models and numerical method

2.1. Inlet model

A model of axial-geometry mixed-compression hypersonic inlet is sketched in Fig. 1. The inlet is designed for a shock-on-lip Mach number of 6.5 and a self starting Mach number of 4.0. The external compression is accomplished by a cone with one turning, for which the initial half angle is 12° and the turning angle is 6°. The internal contraction ratio equals 1.49. Downstream of the throat, a three-dimensional variable section duct for which the area ratio of exit to throat is 1.19, has been adopted.

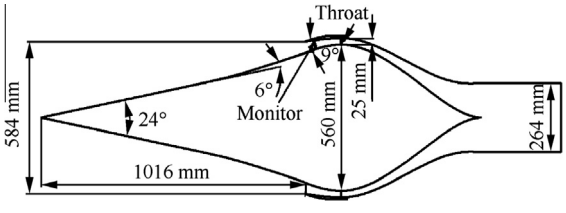

Fig. 1 Schematic diagram of the inlet model.

2.2. Numerical method

The flow was computed by solving the full Navier–Stokes equations. An implicit algorithm with second-order spatial accuracy and dual time-stepping is used for the computation of transient flow field. Multigrid convergence acceleration is employed and the transient flow field is converged at every global time step. The fluid is treated as compressible perfect gas with composition of standard air. The shear-stress transport (SST) two-equation Reynolds averaged Navier–Stokes (RANS) model is used for turbulence modeling. The body surfaces of the inlet are assumed to be no-slip and adiabatic.

The variable laws of inflow parameters with time are controlled by defined functions. Residuals are continuously monitored for continuity, k, ω, axial-velocity, and radial-velocity. The convergence criterion is that all of these residuals are dropped below 10^{-3} with the mass flow rate and the Mach number of mass-weighted average at throat of inlet retaining constant.

2.3. Example of verification

The experiment, which is implemented by Izumi et al.[18] for studying the focusing process of shock waves reflected from parabolic reflectors, is employed to verify the unsteady treatment ability of the numerical method. The shape of the parabolic reflector is expressed by $X = CY^2$, and the C equals 0.5. The incident shock Mach number $Ma = 1.5$. The flow patterns at different moments are shown in Fig. 2, in which the upper pictures are the experimental data and the lower pictures are the computational results. The time t' is nondimensionalized with respect to $\gamma^{1/2}D/\alpha_1$, where γ is specific heats ratio, D is the diameter of parabolic reflector and α_1 is the speed of sound in air ahead of the incident shock. It indicates that the numerical results agree well with the experimental results so the numerical method adopted in this study could describe the unsteady process of complex flow.

2.4. Computational mesh and boundary conditions

The flow of an axial-inlet is axisymmetric when the freestream attack angle is set to 0°, so the two-dimensional axisymmetric computation method is used in this study.

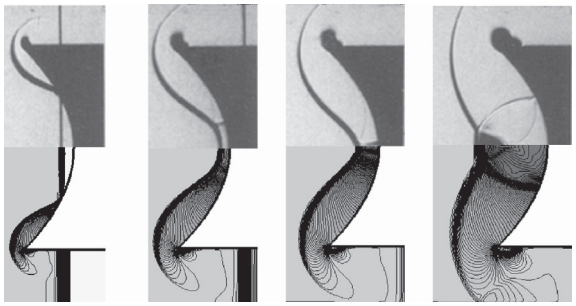

Fig. 2 Comparison of experiment (upper picture) with computation (lower picture).

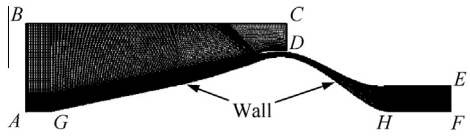

Fig. 3 Computational domain and mesh.

Table 1 Parameters of freestream.

Altitude (km)	Mach number	Static pressure (Pa)	Static temperature (K)
16.0	3.85	10353	216.65
16.0	4.00	10353	216.65
18.5	4.50	6995	216.65
20.0	5.00	5529	216.65
22.0	5.50	4047	218.57
24.0	6.00	2971	220.56
27.0	6.50	1880	223.50

The computational domain and mesh for two-dimensional axisymmetric computation are sketched in Fig. 3.

The grids near the solid wall, where the viscous effect is important, are tightened. AB and BC segments are assigned with pressure far-field, and the freestream parameters are shown in the Table 1. CD and EF are the outflow boundary where a zero gradient extrapolation is applied. AG and HF are the axes.

The grid has some influence on the flow field and performance of inlet, so a grid refinement study is necessary. Prior the study of unsteady starting of inlet, the analysis of gird independence is implemented. Five sets of meshes with different minimum spacing near the wall and numbers of mesh points are generated and their parameters are shown in Table 2.

The time histories of mass flow rate at throat of inlet during impulse starting at Mach number of 6.5 are shown in Fig. 4, from which can be found that the mesh influences the starting process (marked with dashed circle). The time t is measured after the computation begins. It can also be found that the results between mesh number 4 and 5 almost have no difference, so the mesh number 4 is chosen.

3. Results and discussion

3.1. Impulse starting process and flow structure of a hypersonic inlet at design condition

The starting process of a hypersonic inlet is unsteady. The starting type can be divided into impulse starting and self starting in general. In this section, the impulse starting of an inlet at

Table 2 Parameters of mesh.

Mesh number	Minimum spacing (mm)	Number of mesh points
1	0.15	54917
2	0.10	75603
3	0.05	97948
4	0.03	175708
5	0.02	210548

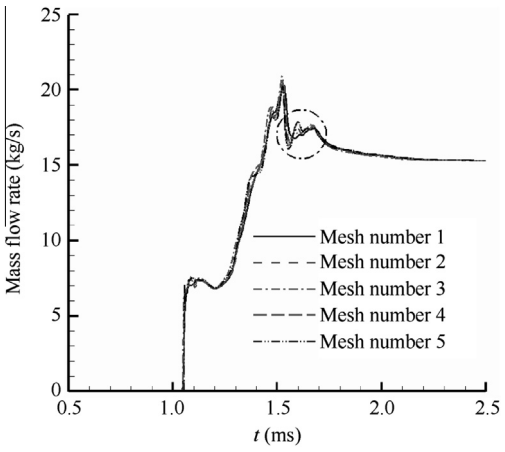

Fig. 4 Time histories of mass flow rate at throat for different meshes.

design condition, i.e., the hypersonic vehicle flies at the altitude of 27 km with the Mach number of 6.5, is investigated. The freestream parameters at design condition, which are used to initialize the whole flow field, are assigned to the pressure far-field boundary of AB and BC. At the initial time (t = 0 ms) of computation, the Mach number of the whole flow field is set to 0, and then the unsteady computation begins.

During impulse starting, the flow field, which is shown in Fig. 5, is divided into three zones along the downstream direction. The gas with high pressure appears between primary shock and upstream-facing shock. The gas downstream of primary shock is stagnant and the gas upstream of upstream-facing shock is the hypersonic test gas. This flow pattern also appears during the impulse wind tunnel starting.[19,20] The stagnant gas swept by primary shock is accelerated greatly, and a supersonic region with high pressure following the primary shock is established. Upstream of the supersonic region is the hypersonic test gas with low pressure and high total temperature, and an upstream-facing shock is formed between the low pressure region and the high pressure region in order to meet the pressure and thermal balance. The starting shock (including primary shock and upstream-facing shock) propagates downstream with time until the inlet starts.

The pressure of the region between primary shock and upstream-facing shock is higher than that of other two regions, but the total temperature decreases from the region of the hypersonic test gas to the stagnant gas. This phenomenon is described with the distributions of pressure and total temperature along the wall in Fig. 6. The pressure p and total temperature T^* are nondimensionalized with respect to the freestream pressure p_0 and temperature T_0 respectively. X is the axial

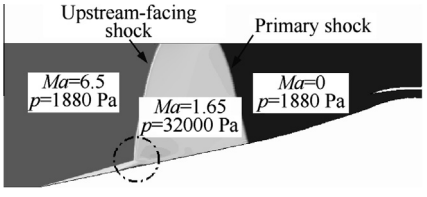

Fig. 5 Mach number contours (t = 0.60 ms).

coordinate. It should be noted that a pressure peak appears at the interface of disturbed gas and test gas. The flow pattern at the foot of primary shock is simple and the primary shock is perpendicular to the wall (see Fig. 5). But the flow pattern at the foot of upstream-facing shock (marked with dashed circle in Fig. 5) is very complex, which is shown in Fig. 7. The conical shock generated by the cone intersects the upstream-facing shock, and this intersection induces the transmitted shock which interacts with boundary layer. The interaction between transmitted shock and boundary layer induces flow separation. The transmitted shock reflects at the wall, which causes the peak pressure. It can be seen from Fig. 8 that the pressure distribution along the wall is variable but similar with time increasing. The high-pressure region between primary shock and upstream-facing shock becomes larger with time increasing because the propagating speed of primary shock is larger than that of upstream-facing shock, and this result is in a good agreement with the experimental data in Ref. [19].

The starting wave system propagates downstream rapidly with time. With time increasing, the separation bubble in the internal duct undergoes a generating, growing, swallowing and disappearing process in sequence. The evolvement of transitional flow field during impulse starting of hypersonic inlet is displayed in Fig. 9.

The primary shock passes through the throat at $t = 1.05$ ms, and the supersonic gas following the primary shock is compressed by cowl lip. During the time from 1.05 ms to 1.40 ms, the oblique shock induced by cowl lip interacts with the boundary layer on the shoulder of ramp, which induces a small separation bubble. This is the generation period of separation bubble. During the period from 1.52 ms to 1.66 ms, the upstream-facing shock sweeps the lip at $t = 1.52$ ms, and the hypersonic test gas flows into the internal duct. So, the oblique shock induced by cowl lip becomes stronger because of the increase of Mach number, which induces larger flow separation. This is the growing period of separation bubble. The gas with high pressure upstream the primary shock passes through throat completely when the time is over 1.66 ms. The separation bubble is swallowed gradually till it disappears. These are the swallowing and disappearing periods of separation bubble, which indicate obviously that the impulse starting process of inlet is unsteady.

The mass flow rate and the Mach number at throat are monitored in order to judge whether the inlet starts or not.

The mass flow rate through the internal duct is unsteady during impulse starting, which can be seen from the time history of mass flow rate at monitor surface and throat in Fig. 10. At one time, the mass flow rate at monitor surface and throat are different, which proves that the mass flow rate is unsteady and does not abide the flow continuity law.

Analyses made on the time history of mass flow rate at throat and the evolvement of flow pattern with time increasing show that the impulse starting process of inlet judged by the flow condition at throat can be divided into three stages in the whole: (1) $t < 1.05$ ms, the gas at throat is stagnant because the primary shock does not reach throat; (2) $t = 1.05$–1.66 ms, during which the gas with high pressure between primary shock and upstream-facing shock passes through throat with the mass flow rate changing greatly. The mass flow rate rises abruptly when the primary shock just sweeps throat at $t = 1.05$ ms. During time increasing from 1.05 ms to 1.52 ms, the mass flow rate increases in the whole with some fluctuation, and the mass flow rate at throat reaches the maximum value at $t = 1.52$ ms. With time increasing, the mass flow rate decreases initially and then

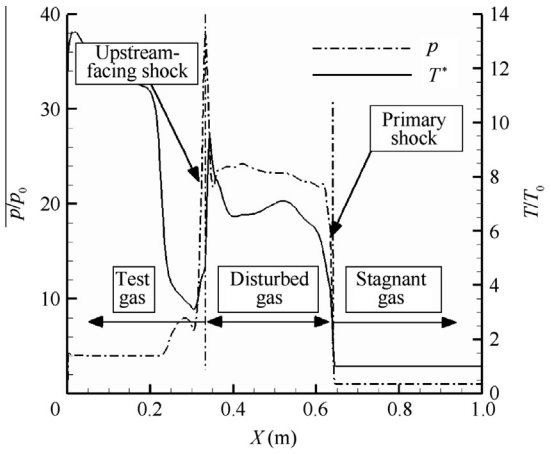

Fig. 6 Distributions of pressure and total temperature along the wall.

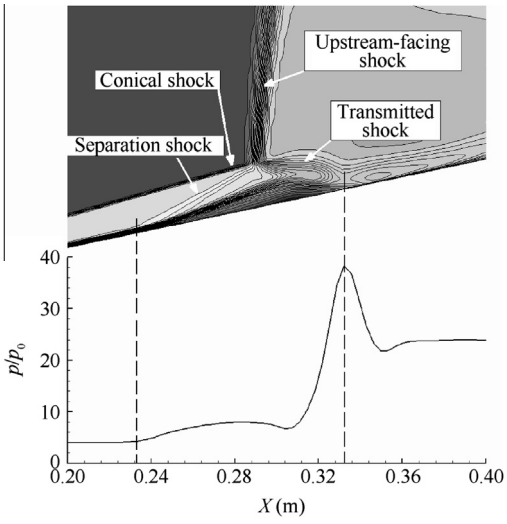

Fig. 7 Shock structure at the foot of upstream-facing shock.

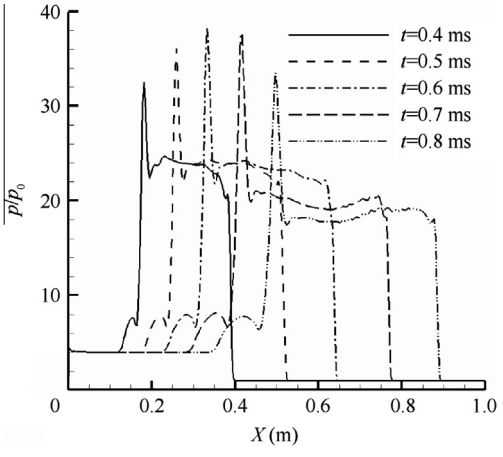

Fig. 8 Pressure distributions along the wall at different time.

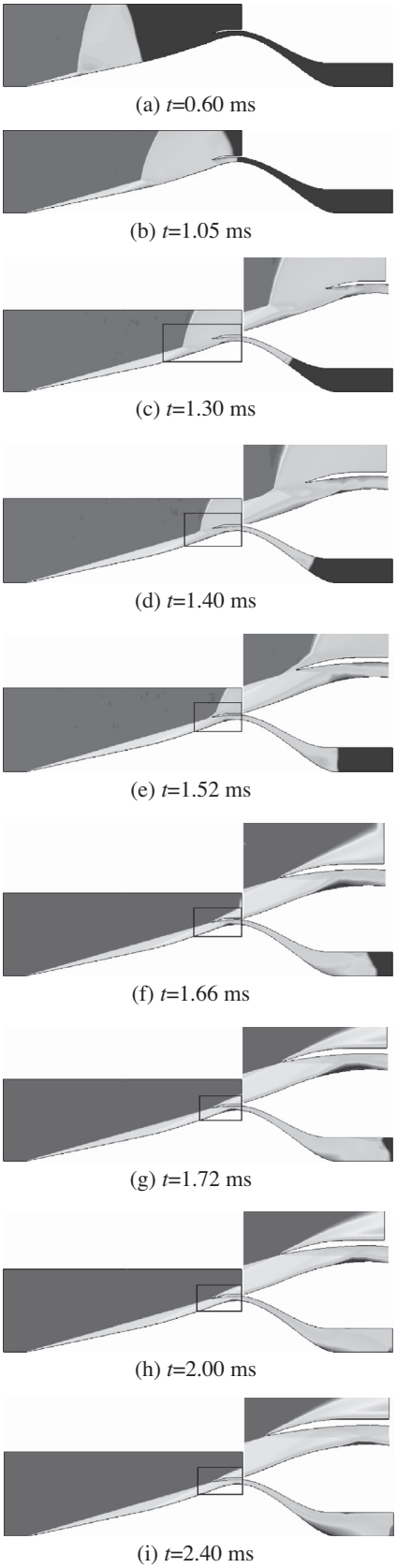

Fig. 9 Transitional flow fields (Mach number contours) at $Ma = 6.5$.

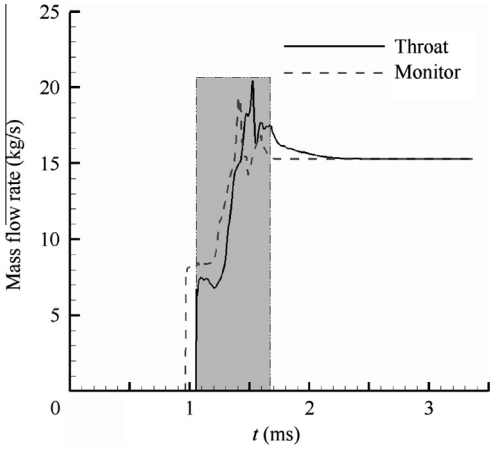

Fig. 10 Time history of mass flow rate at throat for $Ma = 6.5$.

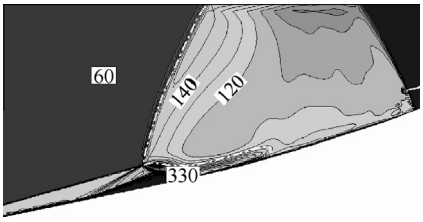

Fig. 11 Mass flux (ρU) contours.

increases slightly from 1.52 ms to 1.66 ms, and the hypersonic test gas fills up throat at $t = 1.66$ ms; (3) the mass flow rate at throat decreases initially after $t = 1.66$ ms, and then remains constant. The whole starting process of inlet lasts 2.4 ms.

During the second stage of impulse starting process, the mass flow rate at throat increases greatly with some fluctuation, which is shown in Fig. 10 with shadow. The mass flux (density ρ multiplied by velocity U) can represent the mass flow rate, and the non-uniform distribution of mass flux leads to the mass flow rate at throat changing greatly. The distribution of mass flux between primary shock and upstream-facing shock is non-uniform with the feature of becoming large gradually from primary shock to upstream-facing shock, and especially the mass flux gradients is large at the interaction zone between transmitted shock and boundary layer (lower-left of the dashed curve), which is displayed with mass flux contours in Fig. 11.

The gas with non-uniform mass flux passes through throat serially, which causes the change of mass flow rate at throat. The evolvement of mass flux contours during impulse starting is shown in Fig. 12. It shows that the primary shock just passes through throat at $t = 1.05$ ms and the mass flow rate rises abruptly. With time increasing, the gas with large mass flux (lower-left of the dashed curve) arrives at throat at $t = 1.20$ ms and the mass flow rate begins to increase. At $t = 1.52$ ms, the gas with largest mass flux passes through throat and the mass flow rate reaches the maximum value. Eventually, the hypersonic test gas fills up throat at $t = 1.66$ ms, and then the starting process enters the third stage.

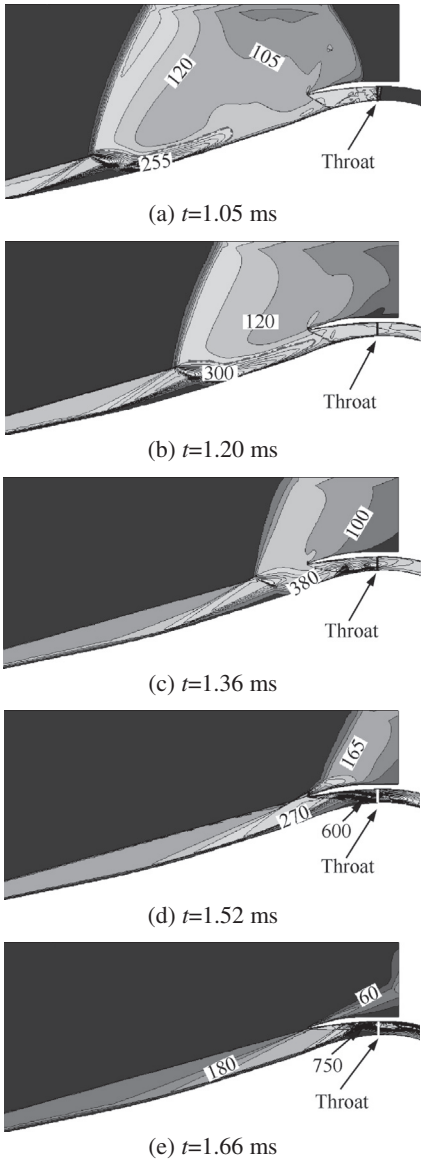

Fig. 12 Mass flux (ρU) contours at different time.

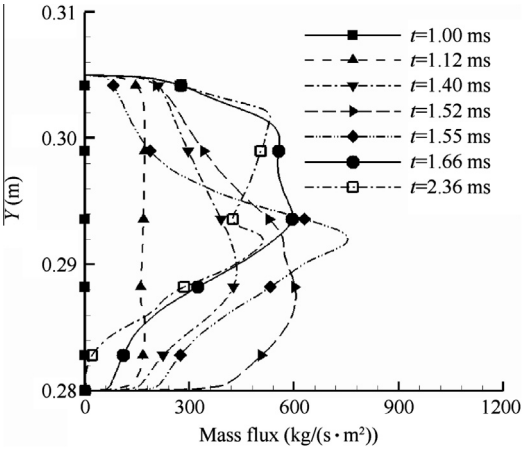

Fig. 13 Distribution of mass flux at throat.

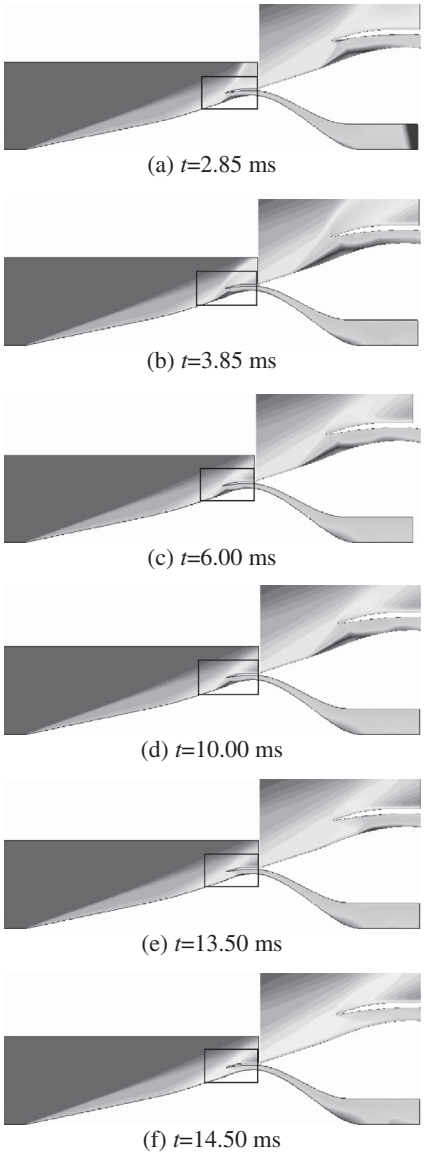

Fig. 14 Transitional flow fields (Mach number contours) at Mach number of 3.85.

The mass flux distribution across throat is unsteady after the primary shock passes through the throat. With time increasing, the mass flux increases in the whole from t = 1.05 ms to 1.52 ms but decreases in the whole from t = 1.52 ms to 2.36 ms, which agrees well with the change of mass flow rate at throat. These are displayed in Fig. 13. In Fig. 13, Y is the radial coordinate of throat.

It can be known that the non-uniform mass flux distribution induced by the interaction between transmitted shock and boundary layer is the main factor which leads to the mass flow rate at throat increasing greatly during the second stage of starting process.

It can be known through the analyses of impulse starting process that the primary shock drives the stagnant gas firstly and this may benefit the inlet stating.

3.2. Influence of freestream Mach number on impulse starting of inlet

The whole impulse starting process at Mach number of 3.85 is similar to that at Mach number of 6.50, which can be seen from the evolvement of transitional flow field during the impulse starting at Mach number of 3.85 in Fig. 14. But the starting duration at Mach number of 3.85 is longer and the detailed flow field differs from that at Mach number of 6.50 obviously. The results show that the separation bubble on the shoulder of ramp undergoes swallowing and disgorging from t = 2.85 ms to 6.00 ms. But the flow field has almost no change from t = 6.00 ms to 10.00 ms because the inlet is working at the critical condition, which leads to the fact that it costs long time for the separation bubble to be swallowed into the inlet. The starting duration at Mach number of 3.85 lasts 14.50 ms.

The time histories of mass flow rate at throat for different freestream Mach numbers are similar and the propagating speed of primary shock becomes slower with the freestream Mach number decreasing, which are shown in Fig. 15. In Fig. 15, H represents the altitude.

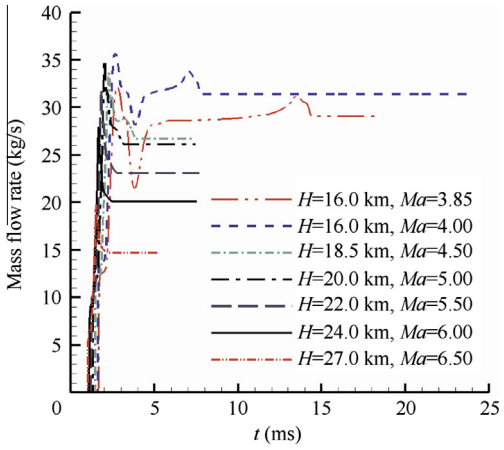

Fig. 15 Time histories of mass flow rate at throat for different freestream Mach number.

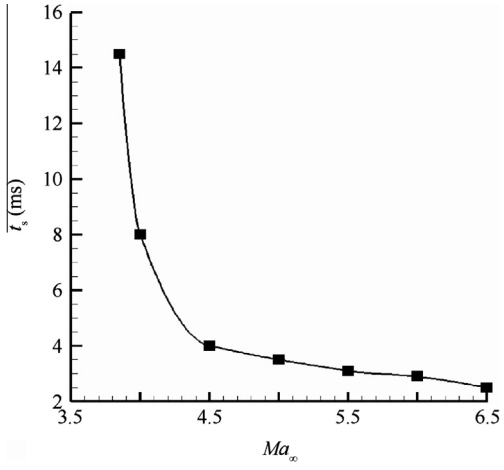

Fig. 16 Starting duration vs freestream Mach number.

The freestream Mach number influences the impulse starting duration of inlet greatly, which is shown in Fig. 16. The variable t_s represents the impulse starting duration. It shows that the impulse starting duration increases almost linearly

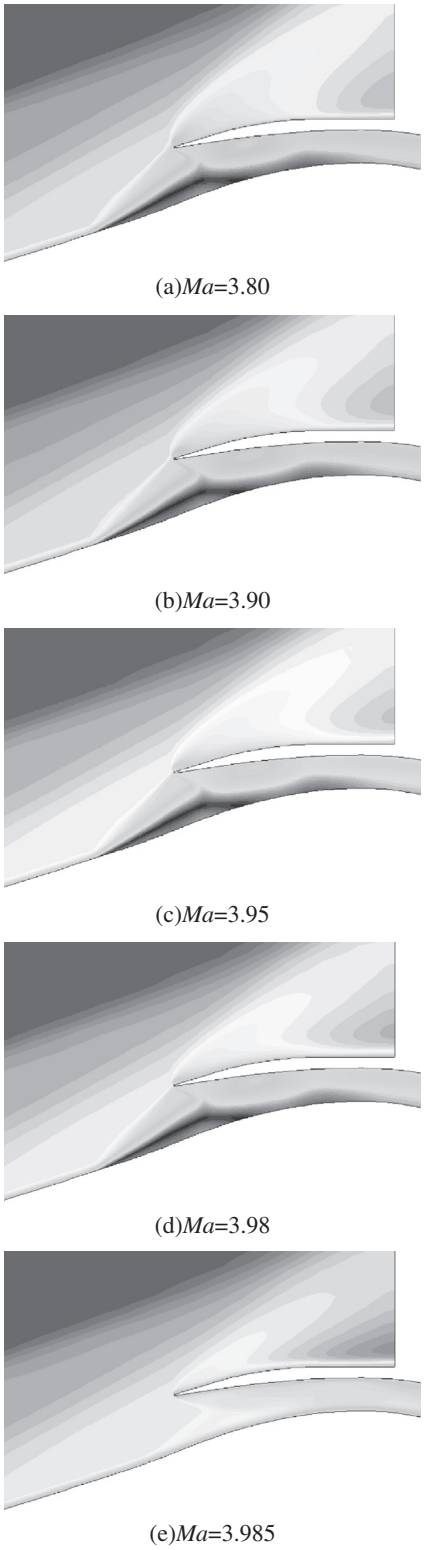

Fig. 17 Mach number contours at different freestream Mach numbers.

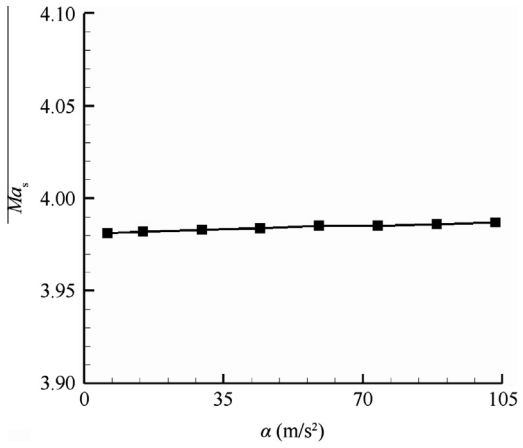

Fig. 18 Effect of accelerating performance of booster on self starting Mach number of hypersonic inlet.

with the decrease of freestream Mach number but rises abruptly when the freestream Mach number approaches the impulse starting Mach number. It is considered that the higher propagating speed of starting shocks (including primary shock and upstream-facing shock) of impulse wind tunnel causes the shorter duration of impulse starting of inlet at high Mach number. Therefore, the requirement to the effective runtime of impulse wind tunnel is different for different freestream Mach numbers, and the false unstarted phenomena of inlet would turn up if the effective runtime of a wind tunnel is too short.

3.3. Influence of accelerating performance of booster on self starting ability of inlet

Apart from impulse starting manner, the self starting is another important starting manner for hypersonic inlet. The self starting of inlet is implemented by the method of accelerating the freestream velocity to the self starting Mach number, so the influence of accelerating performance of booster on the self starting ability of inlet should be given more attention. At the altitude of 16.0 km, the effect of accelerating performance of booster on the self starting ability is numerically studied based on the unstarted quasi-stable flow field at Mach number of 3.80. The unsteady computational fluid dynamics method is applied and the variable law of Mach number with time is assumed linearly.

With time increasing, the freestream Mach number increases and the external compression wave moves close to the lip gradually, which are displayed in Fig. 17. During self starting, a separation bubble on the shoulder of ramp exists until the freestream Mach number is accelerated to the starting Mach number of 3.985. Once the freestream velocity is accelerated to the starting Mach number, the separation bubble disappears immediately and the inlet starts. The flow field exhibits a sudden change during self starting process.

The accelerating performance of booster has almost no influence on the self starting Mach number of inlet, which can be seen in Fig. 18. The variable α and Ma_s represent acceleration and self starting Mach number respectively.

4. Conclusions

(1) The impulse starting and the self starting of hypersonic inlet are unsteady.
(2) During the impulse starting of inlet, the flow field is divided into three zones by primary shock and upstream-facing shock. The primary shock drives the stagnant gas in the inlet firstly, which may benefit the inlet starting. The separation bubble on the shoulder of ramp undergoes a generating, growing, swallowing and disappearing process in sequence.
(3) During the impulse starting of inlet, the non-uniform distribution of mass flux induced by the interaction between transmitted shock and boundary layer causes a large change of mass flow rate at throat.
(4) A separation bubble on the shoulder of ramp exists until the freestream velocity is accelerated to the self starting Mach number during the self starting of inlet.
(5) The duration of impulse starting increases almost linearly with the decrease of freestream Mach number but rises abruptly when the freestream Mach number approaches the starting Mach number.
(6) The accelerating performance of booster almost has no influence on the self-starting ability of inlet.

References

1. Tahir RB. *Starting and unstarting of hypersonic air inlet: an illustrated guide to flow starting phenomena in the axisymmetric busemann geometry and other perforated diffusers*. Saarbrücken: VDM Verlag; 2009.
2. Van Wie DM, Kwok FT, Walsh RF. Starting characterisitics of supersonic inlets. AIAA-1996-2914; 1996.
3. ISGoldberg TJ, Hefner JN. Starting phenomena for hypersonic inlets with thick boundary layers at Mach 6. NASA-TN-D6280; 1971.
4. Huebner LD, Rock KE, Ruf EG, Witte DW, Andrews EH. Hyper-X flight engine ground testing for flight risk reduction. AIAA-2001-1809; 2001.
5. Mayer DW, Paynter GC. Prediction of supersonic inlet unstart caused by freestream disturbances. *AIAA J* 1995;**33**(2):266–75.
6. Andrews EH, McClinton CR, Pinckney SZ. Flowfield starting characteristics of an axisymmetric mixed-compression inlet. NASA-TM-X-2072; 1971.
7. Smart MK. Experimental testing of hypersonic inlet with rectangular-to elliptical shape transition. *J Propul Power* 2001;**17**(2):276–83.
8. Liang DW, Yuan HC, Zhang XJ. Research on the effects of start ability of hypersonic inlet. *J Astronaut* 2006;**27**(4):714–9 [Chinese].
9. Tan HJ, Guo RW. Experimental study of the unstable-unstarted condition of a hypersonic inlet at Mach 6. *J Propul Power* 2007;**23**(4):783–8.
10. Tan HJ, Sun S. Oscillatory flows of rectangular hypersonic inlet unstart caused by downstream mass-flow choking. *J Propul Power* 2009;**25**(1):138–47.
11. Scott DH. Wind-tunnel blockage and actuation systems test of a two-dimensional scramjet inlet model at Mach 6. NASA-TM-109152; 1994.
12. Wang WX, Yuan HC, Huang GP, Liang DW. Impact of suction position on starting of hypersonic inlet. *J Aerosp Power* 2009;**24**(5):918–24 [Chinese].

13. Molder S, Timofeev EV, Tahir RB. Flow starting in high compression hypersonic air inlets by mass spillage. AIAA-2004-4130; 2004.
14. Tahir RB, Molder S, Timofeev EV. Unsteady starting of high Mach number air inlets-a CFD study. AIAA-2003-5191; 2003.
15. Ogawa H, Grainger AL, Bpyce RR. Inlet starting of high-contraction axisymmetric scramjets. AIAA-2009-7401; 2009.
16. Baig S, Timofeev E. A simple moving boundary technique and its application to supersonic inlet starting [dissertation]. Mcgill: Mcgill University; 2008.
17. Timofeev EV, Tahir RB, Molder S. On recent developments related to flow starting in hypersonic air intakes. AIAA-2008-2512; 2008.
18. Izumi K, Aso S, Nishida M. Experimental and computational studies focusing processes of shock waves reflected from parabolic reflectors. *Shock Waves* 1994;**3**(3):213–22.
19. Jacobs PA. Transient, hypervelocity flow in an axisymmetric nozzle. NASA-CR-187496; 1991.
20. Jacobs PA. Simulation of transient flow in a shock tunnel and a high Mach number nozzle. NASA-CR-18706; 1991.

Wang Weixing received B.S. and M.S. degrees in power engineering and aerospace propulsion theory and engineering from Nanjing University of Aeronautics and Astronautics in 2006 and 2008, respectively, and now he is pursuing his Ph.D. degree there. His main research interest is hypersonic aerodynamics.

Guo Rongwei is a professor of Nanjing University of Aeronautics and Astronautics. His main research interests are internal flow aerodynamics and stealth technology.